



Supplement of

Rethinking the role of transport and photochemistry in regional ozone pollution: insights from ozone concentration and mass budgets

Kun Qu et al.

Correspondence to: Xuesong Wang (xswang@pku.edu.cn) and Yuanhang Zhang (yhzhang@pku.edu.cn)

The copyright of individual parts of the supplement might differ from the article licence.

Contents

Three texts, nine figures and two tables are included in this Supporting Information for the paper entitled “Rethinking the role of transport and photochemistry in regional ozone pollution: Insights from ozone mass and concentration budgets”.

Texts:

- Text S1 describes the detailed processes of O₃ budget calculations in this study.
- Text S2 compares the equations of O₃ concentration budget calculations used in this study with these in 1-D models (Eq. (1) in the manuscript).
- Text S3 presents the results of model validation of atmospheric boundary layer (ABL) height, wind and O₃ mixing profiles based on the IAGOS dataset.

Figures:

- Figure S1 indicates two calculation paths for the regional O₃ concentration budget within an hour.
- Figure S2 shows the comparison between IAGOS and modelling atmospheric boundary layer height in Hong Kong during the daytime of Oct. 2015.
- Figure S3 compares IAGOS and modelling wind roses in three height ranges (0-1 km, 1-2 km and 2-5 km) in Hong Kong during the two representative months.
- Figure S4 compares IAGOS and CMAQ modelling vertical profiles of O₃ mixing ratios in Hong Kong during the two representative months.
- Figure S5 presents the spatial distributions of 18 sites of the Guangdong-Hong Kong-Macao Pearl River Delta (PRD) Regional Air Quality Monitoring Network.
- Figure S6 compared the mean diurnal changes of O₃ concentrations in the PRD from three sources: observational near-ground O₃ concentrations, modelled near-ground O₃ concentrations and ABL-mean O₃ concentrations.
- Figure S7 displays the spatial distributions of mean contributions of vertical exchange through the ABL top due to advection perpendicular to the ABL top and its slope (ABL_{ex}-A) to O₃ mass changes in the morning and afternoon of two representative months.
- Figure S8 is the flow diagram of the O₃ budget calculation processes.
- Figure S9 is the flow diagram of the O₃ budget calculation in Step I (or the post-processing tool *flux_4d_cal*).

Tables:

- Table S1 gives more detailed information on the O₃ polluted days of the PRD in the two representative months.
- Table S2 lists the formulas in the O₃ budget calculations, the parameters used and their corresponding source files in the *flux_4d_cal* tool.

Text S1. Detailed processes of O₃ budget calculations

As the flow diagram shown in Fig. S8, there are two steps in the calculations of O₃ budgets based on the WRF-CMAQ modelling results:

1) Step I: Quantifications of process contributions to O₃ mass and volume changes

The post-processing tool *flux_4d_cal* was developed using FORTRAN90 for this step. For all grid columns in d02 except for these adjacent to the boundaries of the modelling domain, the following contents are calculated by the tool:

- Hourly contributions of horizontal transport to O₃ mass changes within the ABL, including these in the x- and y-directions;
- Hourly contributions of vertical exchange due to the changes of ABL height (ABLex-H) to O₃ mass changes within the ABL;
- Hourly contributions of vertical exchange due to advection perpendicular to the ABL top and its slope (ABLex-A) to O₃ mass changes within the ABL, including these in the x-, y- and z-directions;
- Hourly contributions of other processes (gas-phase chemistry, cloud process and dry deposition) to O₃ mass changes within the ABL;
- Hourly transported air volumes by each transport process;
- Total O₃ masses within the ABL at both the start and end of each hour;
- ABL heights at the starting and end hours.

All of the above values can be found in the NetCDF (nc) output files, and they are used in the Step II calculations.

To finish the calculations of Step I, several input files are needed:

- Meteorological files processed by the MCIP module in CMAQ from the WRF outputs, which include the METCRO2D (meteorological parameters in the 2-D space), METCRO3D (meteorological parameters in the 3-D space) and MERDOT3D (wind speeds in the 3-D space) files;
- Pollutant concentration output files (CONC files) modelled by CMAQ, where hourly instantaneous O₃ concentrations are stored;
- Process Analysis (PA) output files modelled by CMAQ, where the hourly, nested contributions of gas-phase chemistry, cloud process and dry deposition to O₃ concentration are stored.

For most of the files used here, the setting of spatial domains and times should be consistent; otherwise, the calculations would not be performed or generate wrong results. Additionally, users should provide the resolution of the modelling domain and the indexes of contributions by three non-transport O₃ processes in the PA files for further calculations.

The flow chart of the calculation in *flux_4d_cal* is shown in Fig. S9. The calculation formulas for the grid column (i, j), parameters used and their source files are summarized in Table S2. There are four loops in the calculations, which are the loops of x-, y-grids, time steps and vertical layers. We assume that there are 60 time-steps within an hour, and parameters at each time step can be interpolated linearly by their values at the starting and end hours. The hourly contribution of non-transport processes to O₃ in a grid cell is divided equally to these within each time step. For every layer within the ABL, contributions to O₃ mass changes and volumes related to horizontal transport and non-transport processes are calculated and summed up to derive the total contributions in the ABL column. For layers where the ABL top is located, besides these aforementioned parameters, contributions to O₃ mass changes and volumes related to vertical exchange (ABLex-H and ABLex-A) are also calculated. Besides, total O₃ masses within the ABL at the start and end of each hour are also calculated, and ABL heights at the starting and end hours can be read from the METCRO2D files.

The height of night-time stable ABL can be severely underestimated by normally used ABL parameterization, especially when the Richardson number is used (Dai et al., 2014). To reduce the influence of imprecise ABL heights in the O₃ budget calculations, here, we set the lowest ABL height limit as 350 m for all hours, which is an approximate value close to the values reported by night-time observations in summer or autumn in the Pearl River Delta (PRD) (Chan et al., 2006; Fan et al., 2011; He et al., 2021; Song et al., 2021). The results of the budget conservation examination (Fig. 3 in the manuscript) also suggest that the choice of this value is acceptable. Further studies are surely needed to determine this value better. However, we focus on the causes of daytime ozone pollution; thus, night-time budgets do not notably influence the conclusions of this study.

2) Step II: Regional O₃ budget calculations and conservation examinations

This step aims to: 1) calculate the hourly O₃ mass and concentration budgets within the ABL of the user-defined regions and 2) check whether the conservation between the changes of O₃ masses/concentrations modelled by CMAQ and the net contributions of O₃-related processes calculated above can be achieved. Besides the nc file generated in Step I, the definition of the grids in user-defined targeted regions, including the border grids and non-border grids, should also be provided by the users. Any software with basic data analysis and nc-file processing functions (Python, MATLAB, R, etc.) can be applied for this step.

The contents in this step include:

- Calculation of hourly contributions of horizontal transport to O₃ mass changes through each user-defined border grid. For horizontal transport through one type of border, its contributions in every interfaces between the border grids of this type and the outside regions, in both x- and y-directions, are summed up as the total contributions of the process in the regional-level O₃ mass budget.

- Calculation of hourly contributions of vertical exchange through the ABL top and other non-transport processes to O₃ mass changes. For one process, its contributions in all grids within the targeted regions are summed up as the total contributions of the process in the regional-level O₃ mass budget.
- Calculation of the hourly O₃ concentration budget (the contributions of O₃-related processes to the hourly variations of mean O₃ concentrations over the ABL of the targeted region) based on the contributions of O₃-related processes to O₃ mass changes and the volumes or volumes changes linked to the processes.

More details on the calculation of the O₃ concentration budget are introduced as follows. As displayed in Fig. S1, within an hour, the mean O₃ concentration within the ABL of the targeted region changes from c_0 to c_1 . During daytime, O₃ mass and ABL volume both change notably, making it difficult to quantify the contributions to O₃ concentration variations by various O₃-related processes. To simplify the calculation, two calculation paths (shown as the red arrow lines in Fig. S1; c_{r1} and c_{r2} are the reference O₃ concentrations separately for two calculation paths) are used in the calculations, assuming that only O₃ mass or ABL volume change in each step of two paths. For the path “ $c_0 \rightarrow c_{r1} \rightarrow c_1$ ”, the first step is the ABL volume change step, with O₃ concentration change described as:

$$c_{r1} - c_0 = c_0 \times \left(\frac{\sum H_0}{\sum H_1} - 1 \right) \quad (S1)$$

where H_0 and H_1 are the ABL heights at the starting and end hours. It is counted as part of the contributions by ABLex-H.

The second step is the O₃ mass change step, with O₃ concentration change described as:

$$c_1 - c_{r1} = \frac{\sum(F_{\text{htrans}} - c_{r1} \times \Delta V_{\text{htrans}})}{L^2 \times \sum H_1} + \frac{\sum(F_{\text{ABLex-A}} - c_{r1} \times \Delta V_{\text{ABLex-A}})}{L^2 \times \sum H_1} + \frac{F_{\text{ABLex-H}}}{L^2 \times \sum H_1} + \frac{F_{\text{chem}}}{L^2 \times \sum H_1} + \frac{F_{\text{cloud}}}{L^2 \times \sum H_1} + \frac{F_{\text{ddep}}}{L^2 \times \sum H_1} \quad (S2)$$

where F_{htrans} , $F_{\text{ABLex-A}}$, $F_{\text{ABLex-H}}$, F_{chem} , F_{cloud} and F_{ddep} indicate the contributions of horizontal transport, ABLex-A, ABLex-H, gas-phase chemistry, cloud process and dry deposition, respectively, to O₃ mass changes; ΔV_{htrans} and $\Delta V_{\text{ABLex-A}}$ are the volumes of transported air parcels attributed to horizontal transport and ABLex-A, respectively, within an hour; L denotes the length of the grid cell, or the horizontal resolution of the model. The six terms on the right-hand side of Eq. (S2) are separately classified as the contributions of horizontal transport, ABLex-A, ABLex-H, gas-phase chemistry, cloud process and dry deposition in the O₃ concentration budgets. Note that the contributions of ABLex-H are separately calculated in two steps, and they are summed up as the total contribution of ABLex-H in the O₃ concentration budget. Similarly, for the path “ $c_0 \rightarrow c_{r2} \rightarrow c_1$ ”, the changes in O₃ concentration in two steps can be described as:

$$c_{r2} - c_0 = \frac{\sum(F_{\text{htrans}} - c_0 \times \Delta V_{\text{htrans}})}{L^2 \times \sum H_0} + \frac{\sum(F_{\text{ABLex-A}} - c_0 \times \Delta V_{\text{ABLex-A}})}{L^2 \times \sum H_0} + \frac{F_{\text{ABLex-H}}}{L^2 \times \sum H_0} + \frac{F_{\text{chem}}}{L^2 \times \sum H_0} + \frac{F_{\text{cloud}}}{L^2 \times \sum H_0} + \frac{F_{\text{ddep}}}{L^2 \times \sum H_0} \quad (S3)$$

$$c_1 - c_{r2} = c_{r2} \times \left(\frac{\sum H_0}{\sum H_1} - 1 \right) \quad (S4)$$

The contributions of various O₃-related processes are classified correspondingly. The final result of individual contribution is estimated as the average value of the contributions calculated based on two calculation paths.

Text S2. Comparisons of the O₃ concentration budget calculations between this study and 1-D models

When the region column in the Chemical Transport Models (CTMs) is thin enough to resemble a line, transport contributions in the O₃ concentration budget calculations based on the CTMs results (Eqs. (6-7) in the manuscript) are expected to have the same forms as these in 1-D models, or Eqs. (1) and (3) in the manuscript:

$$\frac{\partial \langle c_{O_3} \rangle}{\partial t} = -\bar{u} \frac{\partial \langle c_{O_3} \rangle}{\partial x} - \bar{v} \frac{\partial \langle c_{O_3} \rangle}{\partial y} - \frac{\partial \overline{c_{O_3}' w'}}{\partial z} + S(O_3) \quad (1)$$

$$-\frac{\partial \overline{c_{O_3}' w'}}{\partial z} = \frac{\Delta c_{O_3}}{H} \frac{\partial H}{\partial t} + \frac{\Delta c_{O_3}}{H} \left(u_h \frac{\partial H}{\partial x} + v_h \frac{\partial H}{\partial y} - w_h \right) \quad (3)$$

where $\langle c_{O_3} \rangle$ is the mean O₃ concentration over the ABL of the studied region; \bar{u} and \bar{v} are the mean horizontal wind speeds in the x- and y-direction; $S(O_3)$ is the total contribution of non-transport processes to O₃ mass changes; Δc_{O_3} is the difference of O₃ concentrations above and within the ABL; H is the ABL height; u_h , v_h and w_h are the ABL-top wind speeds in the x, y and z-direction, respectively. Thus, we can use it to check the validity of the O₃ concentration budget calculations in this study.

Here the contributions of horizontal transport to the variations of $\langle c_{O_3} \rangle$ can be described as (Eq. (6) in the manuscript):

$$\left[\frac{\partial \langle c_{O_3} \rangle}{\partial t} \right]_{htrans} = \frac{F_{htrans} + \langle c_{O_3} \rangle (V - dV)}{V} - \langle c \rangle = \frac{F_{htrans} - \langle c_{O_3} \rangle dV}{V} \quad (S5)$$

where F_{htrans} is the contributions of horizontal transport to O₃ mass changes; V is the original volume of the PRD grids below the ABL; dV is the volume of transported parcels. Assume that the length of the region in the x-direction is dx , thus,

$$V = S dx \quad (S6)$$

where S is the area of the interface. As calculated in the O₃ mass budget, in the unit time,

$$F_{htrans} = \langle c_{O_3} \rangle_{trans} u L \quad (S7)$$

$$dV = \bar{u} S \quad (S8)$$

where $\langle c_{O_3} \rangle_{trans}$ is the O₃ concentration in the transported air parcels, and. Therefore, from Eqs. (S5)-(S8), we can get:

$$\left[\frac{\partial \langle c_{O_3} \rangle}{\partial t} \right]_{htrans} = \bar{u} \frac{\langle c_{O_3} \rangle_{trans} - \langle c_{O_3} \rangle}{dx} = -\bar{u} \frac{d \langle c_{O_3} \rangle}{dx} \quad (S9)$$

which is the same as the first term on the right side of Eq. (1) in the manuscript. Similarly, the contribution of horizontal transport in the y-direction can be expressed as the second term on the right side of Eq. (1) in the manuscript.

For ABLe_x-H, its contributions when V is much higher than dV (this assumption can be normally met when the period is short) are:

$$\left[\frac{\partial \langle c_{O_3} \rangle}{\partial t} \right]_{ABLe_x-H} = \frac{F_{ABLe_x-H} + \langle c_{O_3} \rangle V}{V + dV} - \langle c_{O_3} \rangle \approx \frac{F_{ABLe_x-H} - \langle c_{O_3} \rangle dV}{V} \quad (S10)$$

where $F_{ABLex-H}$ is the O_3 mass change attributed to ABLex-H. In the unit time,

$$F_{ABLex-H} = c_h \frac{\partial H}{\partial t} L^2 \quad (S11)$$

$$dV = \frac{\partial H}{\partial t} L^2 \quad (S12)$$

$$V = HL^2 \quad (S13)$$

where c_h is the O_3 concentration above the ABL; L is the width of the grid cell (equal to the horizontal resolution of the model). Therefore, from Eqs. (S10)-(S13),

$$\left[\frac{\partial \langle c_{O_3} \rangle}{\partial t} \right]_{ABLex-H} = \frac{c_h - \langle c_{O_3} \rangle}{H} \frac{\partial H}{\partial t} = \frac{\Delta c_{O_3}}{H} \frac{\partial H}{\partial t} \quad (S14)$$

where Δc_{O_3} is the difference of O_3 concentrations above and within the ABL ($c_h - \langle c_{O_3} \rangle$). Apparently, it is the same as the first term on the right side of Eq. (3) in the manuscript.

For ABLex-A,

$$\left[\frac{\partial \langle c_{O_3} \rangle}{\partial t} \right]_{ABLex-A} = \frac{F_{ABLex-A} + \langle c_{O_3} \rangle (V - dV)}{V} - \langle c_{O_3} \rangle = \frac{F_{ABLex-A} - \langle c_{O_3} \rangle dV}{V} \quad (S15)$$

$F_{ABLex-M}$ is the contributions of ABLex-A to O_3 mass change. In the unit time,

$$F_{ABLex-A} = c_h \left(u_h \frac{\partial H}{\partial x} + v_h \frac{\partial H}{\partial y} - w_h \right) L^2 \quad (S16)$$

$$dV = \left(u_h \frac{\partial H}{\partial x} + v_h \frac{\partial H}{\partial y} - w_h \right) L^2 \quad (S17)$$

$$V = HL^2 \quad (S18)$$

Therefore, from Eq. (S15-18),

$$\left[\frac{\partial \langle c_{O_3} \rangle}{\partial t} \right]_{ABLex-A} = \frac{c_h - \langle c_{O_3} \rangle}{H} \left(u_h \frac{\partial H}{\partial x} + v_h \frac{\partial H}{\partial y} - w_h \right) = \frac{\Delta c_{O_3}}{H} \left(u_h \frac{\partial H}{\partial x} + v_h \frac{\partial H}{\partial y} - w_h \right) \quad (S19)$$

It is the same as the second term on the right side of Eq. (3) in the manuscript.

Based on the above discussion, for the contributions of all transport processes considered in the O_3 budget calculations, the above formulas (Eqs. (S9), (S14) and (S19)) are the same as those used in 1-D models (Janssen and Pozzer, 2015; Vilà-Guerau de Arellano et al., 2015), suggesting their applicability in the quantification of the O_3 concentration budget using CTMs modelling results.

Text S3. Model validation of ABL height, wind and O₃ mixing ratio profiles based on the IAGOS dataset

IAGOS (In-service Aircraft of a Global Observing System; <https://www.iagos.org>) is a global aircraft-based observing system, where state-of-the-art instruments deployed in aircraft are used to measure reactive gases, greenhouse gases, aerosol and clouds in the troposphere and lower stratosphere (Petzold et al., 2016). Meteorological parameters, including air temperature, wind speed and direction, are also provided by IAGOS. When the aircraft climb up or descend, these measurements are suitable for obtaining the vertical profiles of parameters with high resolutions, which provides valuable observational datasets for the model validation in the vertical direction.

To ensure reasonable quantifications of the O₃ budgets, the IAGOS dataset in two representative months in Hong Kong (located in the south PRD) was used to evaluate the modelling performance of WRF-CMAQ in this study. We focused on comparing parameters within the height range of 0-5 km. Since observational data is often missing in some height ranges and the vertical resolution of modelling results is relatively low, for the temperatures, wind speeds and directions at different heights, we calculated their mean observational and modelling values within every 500 m height range (i.e., 0-500 m, 500-1000 m, etc.) as the data used in the comparisons. The detailed evaluations are introduced as follows:

(1) Atmospheric boundary layer (ABL) heights:

ABL height is an important parameter in the O₃ budget calculations — it is used in the quantification of the contributions from all O₃-related processes. Therefore, a good modelling performance of ABL height is important for accurately analyzing O₃ budgets. In this study, the observational ABL heights were determined using the profiles of potential temperature (θ) in IAGOS, and they are defined as the heights where the lapse rate of θ ($\partial\theta/\partial z$, the rate of θ changing over height change) reaches its maximum values (Dai et al., 2014). Since there are limited profiles available in July 2016 and night-time ABL heights are hard to be determined accurately, we only evaluated the modelling performance of ABL heights during the daytime (6:00-18:00 Local Time (LT)) of Oct. 2015. As shown in Fig. S2, the mean bias (MB) between modelling and observational ABL heights in Hong Kong is only -1.1 m, and a good correlation between ABL heights from two datasets ($R = 0.76$) suggests that the mean diurnal cycles of ABL during daytime can be modelled well. Though the modelling performance of ABL heights is satisfying based on the IAGOS dataset in Hong Kong, more comprehensive comparisons based on three-dimensional observations with higher spatiotemporal resolutions and coverages are still required for more accurate O₃ budget estimates in future studies.

(2) Wind profiles:

Figure S3 shows the IAGOS and modelling wind roses within the height ranges of 0-1000 m, 1000-2000 m and 2000-5000 m. Both datasets indicate that higher wind speeds can be generally found at higher altitudes. In autumn, WRF overestimates wind speed below 1000 m by 0.6 m/s (16%) but underestimates it above 1000 m. In summer, the biases between wind speeds

in the two datasets are relatively smaller, especially at lower heights (< 2000 m). Both datasets show similar prevailing wind directions at different height ranges and seasons. Thus, the modelling performance of wind speeds and directions in the vertical direction is acceptable.

(3) O₃ mixing ratio profiles:

The comparisons between observational and modelling profiles of the O₃ mixing ratio are displayed in Fig. S4. Few O₃ profiles were available in July 2016, and the useable ones were mostly measured during clean periods. Thus, the comparison was mainly based on the results in Oct. 2015 (the number of IAGOS O₃ profiles available for the comparisons is 41). Both datasets show that the O₃ mixing ratio decreases with height in Hong Kong. Below the height of 1000 m, the observational and modelling O₃ mixing ratios are 71.4 ppbv and 75.8 ppbv, respectively. Within the height range of 1000-2000 m, the O₃ mixing ratio is overestimated by 26%. High O₃ levels during Oct. 13-24 and relatively low O₃ levels in other periods can be found in both datasets, suggesting that the development, maintenance and dissipation of O₃ pollution in this month were modelled well. Therefore, the performance of O₃ profile modelling can also meet the requirement of O₃ budget calculations.

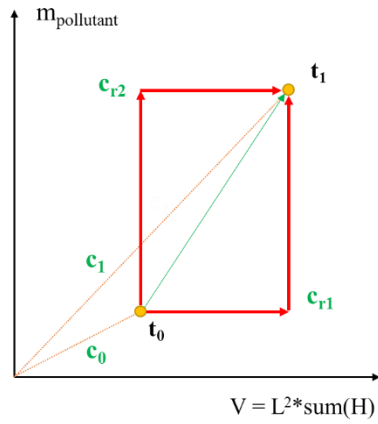


Figure S1. Two calculation paths for the regional-level O₃ concentration budget within an hour. $m_{\text{pollutant}}$ indicates the total mass of pollutants in the atmospheric boundary layer (ABL) of the studied region; V is the volume of the ABL of the targeted region; L is the length of the grids (equal to the horizontal resolution of the model); H is the ABL heights; t_0 and t_1 are the starting and end hour, respectively; c_0 and c_1 are the concentrations of pollutants in t_0 and t_1 , respectively; c_{r1} and c_{r2} are the reference concentrations of pollutants for two calculation paths.

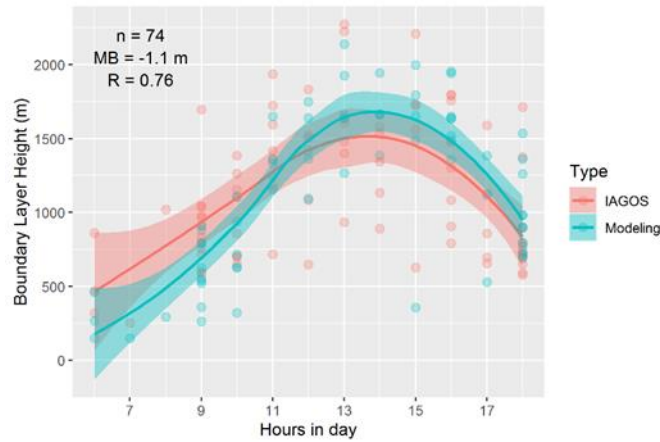


Figure S2. Comparisons between IAGOS and modelling atmospheric boundary layer height in Hong Kong during the daytime of Oct. 2015. n , the number of the available data pairs for the comparison; MB , mean bias; R , correlation factor.

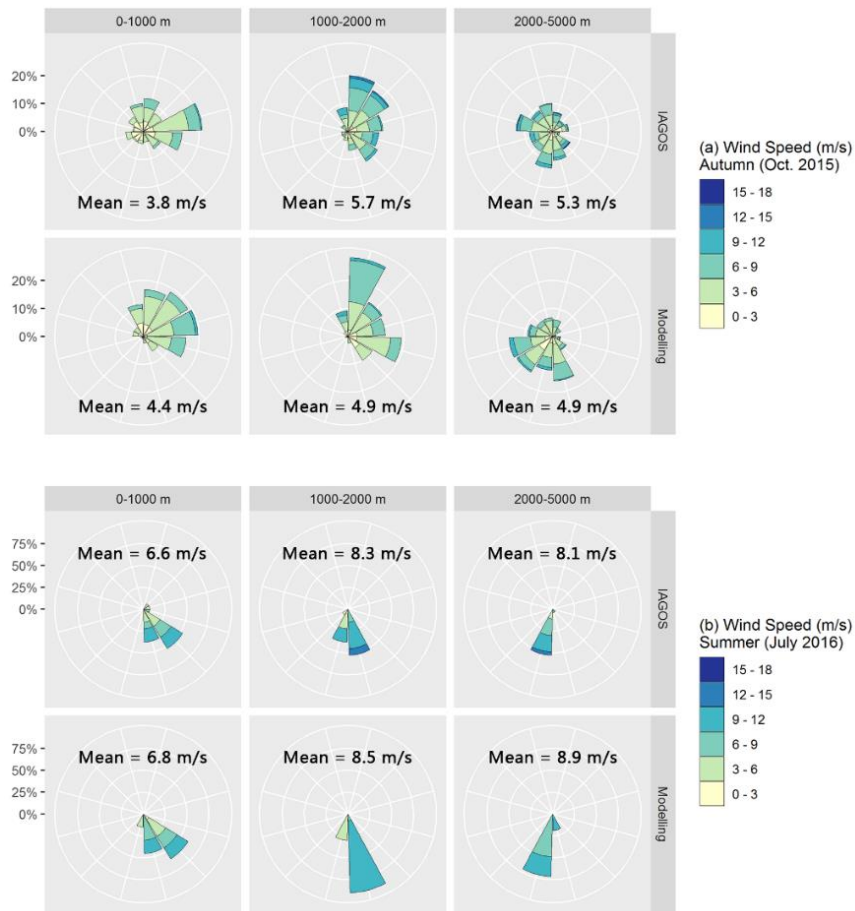


Figure S3. Comparisons between IAGOS and modelling wind roses in Hong Kong in (a) Oct. 2015 and (b) July 2016. Results within the height range of 0-1000 m, 1000-2000 m, and 2000-5000 m were separately displayed.

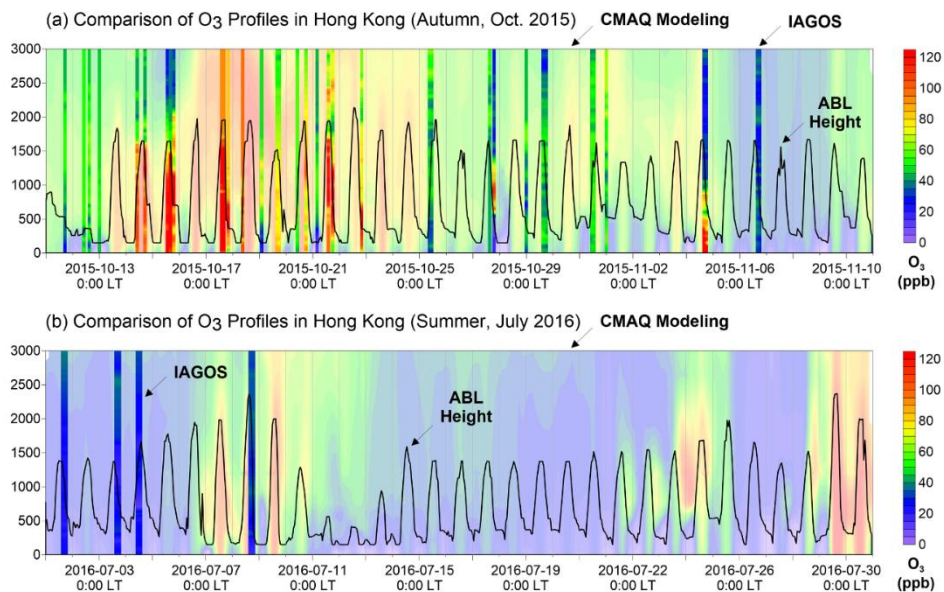


Figure S4. Comparisons between IAGOS and CMAQ modelling vertical profiles of O₃ mixing ratios (ppb) in Hong Kong in (a) Oct. 2015 and (b) July 2016. The heights of the atmospheric boundary layer (ABL) modelled by WRF in two representative months are shown as solid black lines.

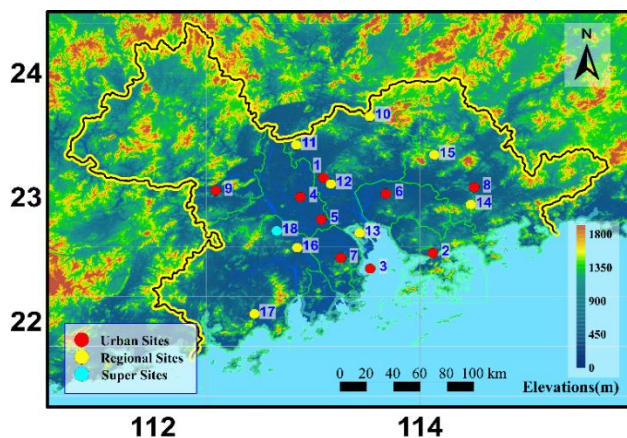


Figure S5. Spatial distributions of 18 sites of the Guangdong-Hong Kong-Macao Pearl River Delta Regional Air Quality Monitoring Network. The names of all sites and the municipalities where they are located are as follows: 1. Luhu, Guangzhou; 2. Liyuan, Shenzhen; 3. Tangjia, Zhuhai; 4. Huijingcheng, Foshan; 5. Jinjuju, Foshan; 6. Nanchengyuanling, Dongguan; 7. Zimaling, Zhongshan; 8. Xiapu, Huizhou; 9. Chengzhongzizhan, Zhaoqing; 10. Tianhu, Guangzhou; 11. Zhudong, Guangzhou; 12. Modiesha, Guangzhou; 13. Wanqingsha, Guangzhou; 14. Jinguowan, Huizhou; 15. Xijiao, Huizhou; 16. Donghu, Jiangmen; 17. Duanfen, Jiangmen; 18. Heshan Supersite, Jiangmen.

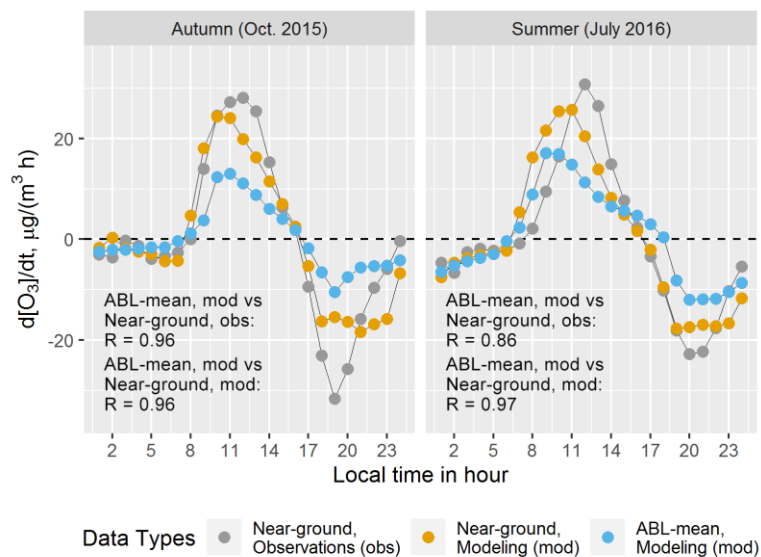


Figure S6. Mean diurnal change of the hourly variations of observational, modelling mean near-ground O₃ concentrations in 18 sites of the Guangdong-Hong Kong-Macao regional monitoring network and modelling mean O₃ concentration over the atmospheric boundary layer (ABL) of the Pearl River Delta on the polluted days of autumn (Oct. 2015) and summer (July 2016). “mod” and “obs” are short for models and observations, respectively; R, correlation factor.

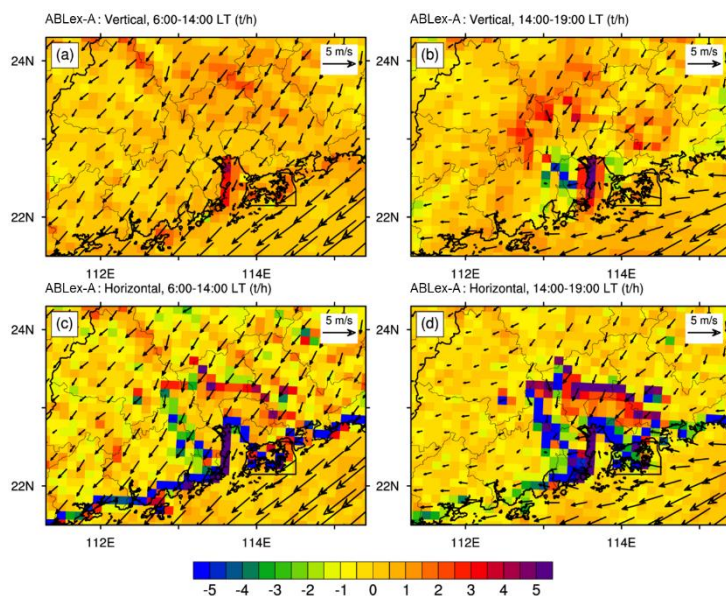


Figure S7. The spatial distributions of contributions of ABLex-A to O₃ mass changes on the polluted days of Oct. 2015. (a-b) Contributions through vertical advection; (c-d) contributions through horizontal advection. (a,c) The mean results during the morning hours (6:00-14:00 LT); (b,d) the mean results during the afternoon hours (14:00-19:00 LT).

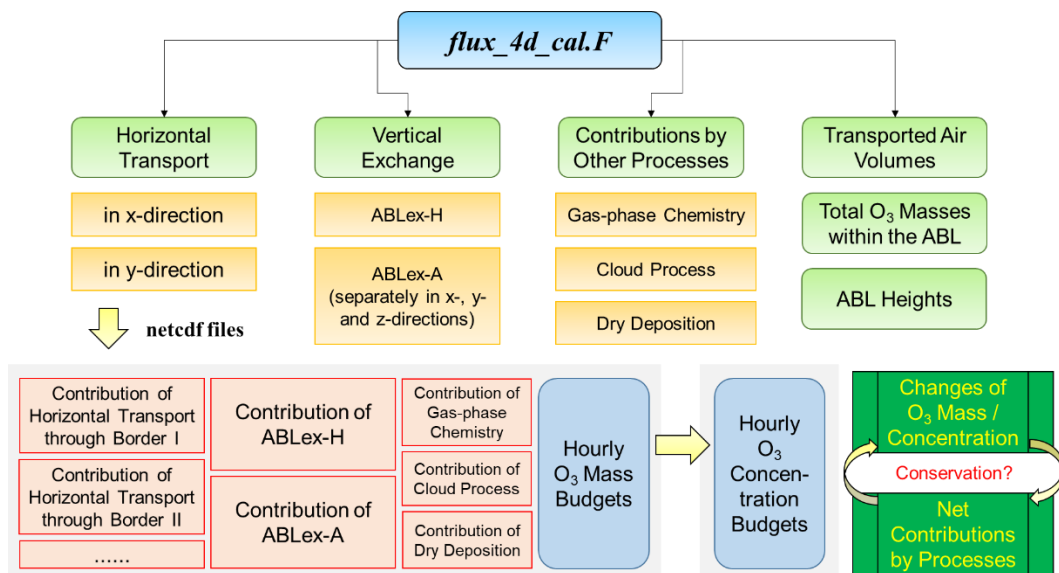


Figure S8. Flow diagram of the O₃ budget calculation processes. ABL, atmospheric boundary layer; ABLex-H, vertical exchange through the ABL top due to the changes of ABL height; ABLex-A, vertical exchange through the ABL top due to advection perpendicular to the ABL top and its slope.

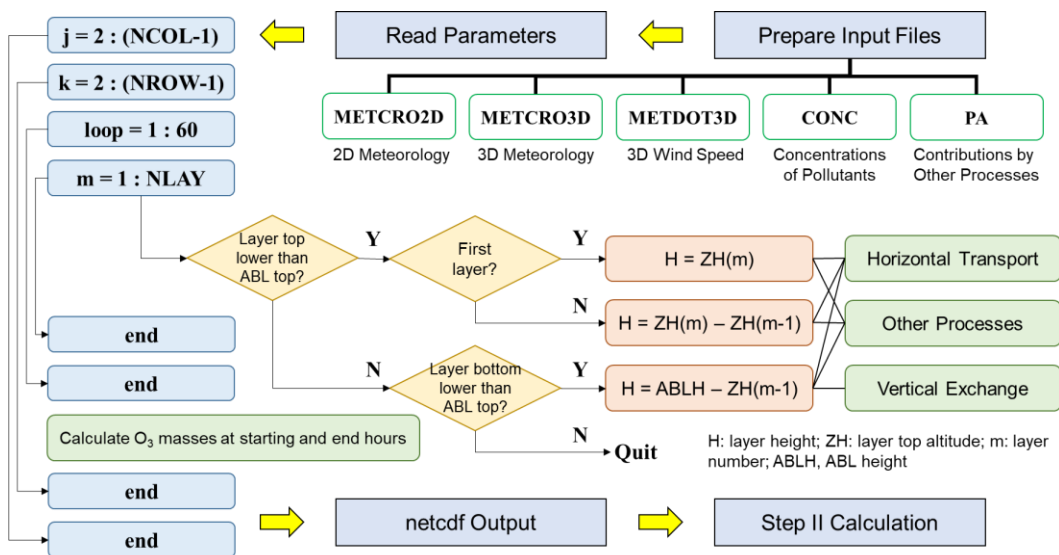


Figure S9. Flow diagram of the O₃ budget calculation in Step I (or the post-processing tool *flux_4d_cal*). NCOL, NROW and NLAY indicate the number of columns, rows and vertical layers in the modelling domain. ABL, atmospheric boundary layer. METCRO2D, 2-dimensional meteorological outputs from the MCIP module in CMAQ; METCRO3D, 3-dimensional meteorological outputs from the MCIP module in CMAQ; METDOT3D, 3-dimensional wind fields outputs from the MCIP module in CMAQ; CONC, 3-dimensional outputs of pollutant concentrations from CMAQ; PA, 3-dimensional outputs of hourly contributions by non-transport processes to O₃ from CMAQ.

Table S1. Information on the O₃ polluted days of the Pearl River Delta (PRD) in Oct. 2015 and July 2016. MDA1, the maximum 1-hr O₃ concentrations; MDA8, the maximum 8-hr average O₃ concentrations.

Dates	Influencing Weather Systems	O ₃ concentrations in the PRD (the maximum values in nine municipals of the PRD, released by the China National Environmental Monitoring Centre; µg/m ³)	
		MDA1	MDA8
Oct.13, 2015		201	164
Oct.14, 2015		301	244
Oct.15, 2015		271	227
Oct.16, 2015		260	219
Oct.17, 2015		233	211
Oct.18, 2015	Typhoon Koppu and Champi	205	187
Oct.19, 2015		214	174
Oct.20, 2015		200	158
Oct.21, 2015		214	195
Oct.22, 2015		209	182
Oct.23, 2015		249	199
Oct.24, 2015		225	193
Oct.28, 2015	Subtropical High	238	186
Nov.3, 2015		207	162
Nov.4, 2015	Sea High	182	168
Nov.5, 2015		255	187
July 7, 2016		297	256
July 8, 2016	Typhoon Nepartak	260	198
July 9, 2016		263	231
July 10, 2016		211	150
July 22, 2016			211
July 23, 2016		223	197
July 24, 2016	Subtropical High	265	226
July 25, 2016		334	269
July 26, 2016		235	164
July 29, 2016		271	204
July 30, 2016			268
July 31, 2016	Typhoon Nida	385	344

Table S2. Formulas in the calculations of process contributions to O₃ mass changes for the grid cell (*i, j*) in the unit time *dt*, parameters used and their source files in the *flux_4d_ccl* tool.

Processes	Formulas to calculate process contributions to O ₃ mass changes	Parameters used	Sources of parameters
Horizontal transport (in the x-direction)	$F_{u-trans} = \sum_{k=1}^h c_{i-1,j} u_{i,j+\frac{1}{2}} L \Delta z dt$	$c_{i-1,j}$: O ₃ concentrations in the grid cell (<i>i-1, j</i>)	CONC files
		$u_{i,j+\frac{1}{2}}$: wind speeds in the west interface	METDOT3D files
		L : the length of grid cells (= model resolution)	User defined
		Δz : layer heights (H - z_{h-1} for the ABL top layer; $z_k - z_{k-1}$ for other layers within the ABL; H, ABL height)	METCRO3D files
Horizontal transport (in the y-direction)	$F_{v-trans} = \sum_{k=1}^h c_{i,j-1} v_{i+\frac{1}{2},j} L \Delta z dt$	$c_{i,j-1}$: O ₃ concentrations in the grid cell (<i>i, j-1</i>)	Determined by ABL height
		$v_{i+\frac{1}{2},j}$: wind speeds in the south interface	CONC files
		L : the length of grid cells (= model resolution)	METDOT3D files
		Δz : layer heights (H - z_{h-1} for the ABL top layer; $z_k - z_{k-1}$ for other layers within the ABL; H, ABL height)	User defined
ABL ex-H	$F_{ABL\text{ex-H}} = c_h \frac{\partial H}{\partial t} L^2 dt$	c_h : O ₃ concentrations in the ABL top layer	Determined by ABL height
		$\frac{\partial H}{\partial t}$: the change rates of ABL height	CONC files
		L : the length of grid cells (= model resolution)	METCRO2D files
		User defined	
ABL ex-A (in the x-direction)	$F_{ABL\text{ex-Ax}} = c_{i-1,j(n)} u_{i,j+\frac{1}{2}(n)} \frac{\partial H}{\partial x} L^2 dt$	$c_{i-1,j(n)}$: O ₃ concentrations in the ABL top layer of the grid cell (<i>i-1, j</i>)	CONC files
		$u_{i,j+\frac{1}{2}(n)}$: wind speeds in the ABL top layer of the west interface	METDOT3D files
		L : the length of grid cells (= model resolution)	User defined
		$\frac{\partial H}{\partial x}$: the difference of ABL heights in x-direction, or between the grid cells (<i>i, j</i>) and (<i>i-1, j</i>)	METCRO2D files
ABL ex-A (in the y-direction)	$F_{ABL\text{ex-Ay}} = c_{i,j-1(n)} v_{i+\frac{1}{2}(n)} \frac{\partial H}{\partial y} L^2 dt$	$c_{i,j-1(n)}$: O ₃ concentrations in the ABL top layer of the grid cell (<i>i, j-1</i>)	CONC files
		$v_{i+\frac{1}{2}(n)}$: wind speeds in the ABL top layer of the south interface	METDOT3D files
		L : the length of grid cells (= model resolution)	User defined
		$\frac{\partial H}{\partial y}$: the difference of ABL heights in y-direction, or between the grid cells (<i>i, j</i>) and (<i>i, j-1</i>)	METCRO2D files
ABL ex-A (in the z-direction)	$F_{ABL\text{ex-Az}} = -c_h w_h L^2 dt$	c_h : O ₃ concentrations in the ABL top layer	CONC files
		w_h : vertical wind speeds in the ABL top layer	METCRO3D files
		L : the length of grid cells (= model resolution)	User defined
		IPR : integrated process rates of pre-set processes	PA files
Other processes (gas-phase chemistry, cloud process, dry deposition)	$F_{others} = \sum_{k=1}^h IPR \Delta z dt$	Δz : layer heights (H - z_{h-1} for the ABL top layer; $z_k - z_{k-1}$ for other layers within the ABL; H, ABL height)	METCRO3D files
		h : the layer of ABL top	Determined by ABL height

References (of the Supplement)

- Chan, R. L. M., Lee, O. S. M., and Cheng, A. Y. S.: Diurnal variation of mixing height in Hong Kong. In Reviewed and revised papers presented at the 23rd International Laser Radar Conference (pp. 737-740), 2006.
- Dai, C., Wang, Q., Kalogiros, J. A., Lenschow, D. H., Gao, Z., and Zhou, M.: Determining Boundary-Layer Height from Aircraft Measurements, *Bound.-Lay. Meteorol.*, 152, 277–302, <https://10.1007/s10546-014-9929-z>, 2014.
- Fan, S. J., Fan, Q., Yu, W., Luo, X. Y., Wang, B. M., Song, L. L., and Leong, K. L.: Atmospheric boundary layer characteristics over the Pearl River Delta, China, during the summer of 2006: measurement and model results, *Atmos. Chem. Phys.*, 11, 6297–6310, <https://doi.org/10.5194/acp-11-6297-2011>, 2011.
- He, G., Deng, T., Wu, D., Wu, C., Huang, X., Li, Z., Yin, C., Zou, Y., Song, L., Ouyang, S., Tao, L., and Zhang, X.: Characteristics of boundary layer ozone and its effect on surface ozone concentration in Shenzhen, China: A case study, *Sci. Total Environ.*, 791, 148044, <https://doi.org/10.1016/j.scitotenv.2021.148044>, 2021.
- Janssen, R. H. H. and Pozzer, A.: Description and implementation of a MiXed Layer model (MXL, v1.0) for the dynamics of the atmospheric boundary layer in the Modular Earth Submodel System (MESSy), *Geosci. Model Dev.*, 8, 453–471, <https://doi.org/10.5194/gmd-8-453-2015>, 2015.
- Petzold, A., Thouret, V., Gerbig, C., Zahn, A., Brenninkmeijer, C. A. M., Gallagher, M., Hermann, M., Pontaud, M., Ziereis, H., Boulanger, D., Marshall, J., Nédélec, P., Smit, H. G. J., Friess, U., Flaud, J.-M., Wahner, A., Cammas, J.-P., Volz-Thomas, A. and IAGOS TEAM: Global-scale atmosphere monitoring by in-service aircraft—current achievements and future prospects of the European Research Infrastructure IAGOS, *Tellus B*, 67, 28452, <https://doi.org/10.3402/tellusb.v67.28452>, 2015.
- Song, L., Deng, T., Li, Z. N., Wu, C., He, G. W., Li, F., Wu, M., and Wu, D. (2021). Retrieval of boundary layer height and its influence on PM_{2.5} concentration based on lidar observation over Guangzhou, *J. Trop. Meteorol.*, 27(3), 303-318, <https://doi.org/10.46267/j.1006-8775.2021.027>, 2021.
- Vilà-Guerau De Arellano, J., van Heerwaarden, C. C., van Stratum, B. J. H., and van den Dries, K.: Atmospheric Boundary Layer: Integrating Air Chemistry and Land Interactions, Cambridge University Press, New York, 2015.